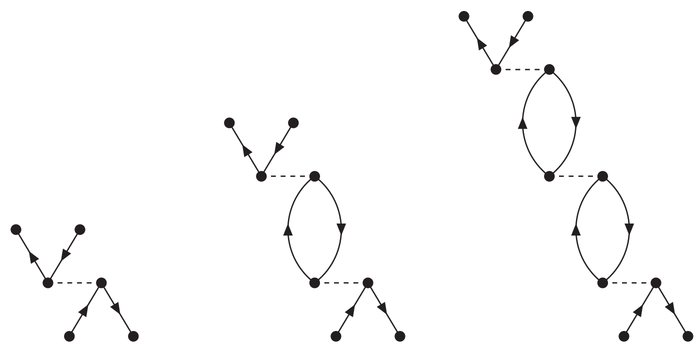

Fig. 14.6 Diagrammatic representation of a few higher-order diagrams generated by Eq. (14.21) when only the direct contribution to V_{ph} is employed as shown in Fig. 14.4. Note that the dashed line in this figure represents the corresponding direct contribution to V_{ph} as defined in Eq. (14.17).

ring, bubble, or sausage diagrams. This name calling becomes clear when the direct contribution to V_{ph} is used to generate the higher-order terms implied by Eq. (14.21). Examples of such diagrams are shown in Fig. 14.6. The bubbles or rings emerge when the direct part of the interaction is used to connect the unperturbed ph propagation as shown in Fig. 14.6. It should be emphasized again that the diagrams displayed in Fig. 14.6 correspond to Feynman diagrams in the energy formulation. Each bubble, for example, represents the sum of a forward- and a backward-going term corresponding to the first or second term of Eq. (14.13), respectively. The presence of both these terms implies an interplay between these components when Eq. (14.21) is solved. The presence of both terms generates the possibility of intermediate states in which many particle-hole states are present at the same time. If no backward-going contributions are present only one particle-hole pair propagates at each moment. One can generate an example of a term with more intermediate particle-hole states by taking one of the bubbles in Fig. 14.6 and flipping it downward. The presence of such contributions implies that some higher-order contributions with more particle-hole intermediate states are included. Other are, however, neglected in particular those in which particles or holes are exchanged with each other. One may argue that these Pauli exchange terms add up with random phases and might therefore be rather small, hence the appearance of the name random phase approximation. General features of the solutions of the RPA equation for the polarization propagator in finite systems will be presented in the next section.

14.3 RPA in finite systems and the schematic model

The solution to Eq. (14.20) starts by assuming that Π^{RPA} also has a Lehmann representation just as the unperturbed and the exact polarization propagator. This assumption implies that the transition amplitudes and excitation energies in principle require a distinct notation since they refer to a specific approximation (RPA) to the polarization propagator. It is convenient to define

$$\mathcal{X}^n_{\alpha\beta} \equiv \left\langle \Psi^A_n \right| a^\dagger_\alpha a_{\overline{\beta}} \left| \Psi^A_0 \right\rangle, \tag{14.22}$$

$$\mathcal{Y}^n_{\alpha\beta} \equiv \left\langle \Psi^A_n \right| a^\dagger_{\overline{\alpha}} a_\beta \left| \Psi^A_0 \right\rangle, \tag{14.23}$$

which are related under time reversal, and

$$\varepsilon^\pi_n \equiv E^A_n - E^A_0, \tag{14.24}$$

keeping in mind that these quantities refer to the RPA description of the polarization propagator. With this notation the corresponding Lehmann representation becomes

$$\Pi^{RPA}(\alpha,\beta^{-1};\gamma,\delta^{-1};E) = \sum_{n\neq 0} \frac{(\mathcal{X}^n_{\alpha\beta})^* \mathcal{X}^n_{\gamma\delta}}{E - \varepsilon^\pi_n + i\eta} - \sum_{n\neq 0} \frac{(\mathcal{Y}^n_{\delta\gamma})^* \mathcal{Y}^n_{\beta\alpha}}{E + \varepsilon^\pi_n - i\eta}. \tag{14.25}$$

In the case of a finite system it is natural to consider bound excited states and, consequently, the summation in Eq. (14.25) indeed involves some discrete states. As a result, this Lehmann represenation includes simple poles. For simplicity one may assume that all excited states correspond to discrete excitation energies. With this assumption one may exploit a technique that was introduced in Ch. 7 (and used several times since) to solve propagator equations with discrete poles. The procedure involves the calculation of

$$\lim_{E\to\varepsilon^\pi_n} (E - \varepsilon^\pi_n)\left\{\Pi^{RPA} = \Pi^{(0)} + \Pi^{(0)}\ V_{ph}\ \Pi^{RPA}\right\}, \tag{14.26}$$

where Eq. (14.21) has been rendered in a schematic fashion. As in Ch. 7, one proceeds by considering the limits for the three terms in Eq. (14.26). Using the Lehmann representation for Π^{RPA}, one immediately obtains the product of two transition amplitudes associated with excited state n for the left hand side of Eq. (14.26). The limit yields no contribution when it is taken for the first term on the right side which involves $\Pi^{(0)}$. One may draw this conclusion whenever the interaction V_{ph} is nonvanishing since its action will imply that the RPA excitation energies will differ from the unperturbed ph energies. Using similar arguments for the final term one arrives at the following eigenvalue equation after cancelling a common factor $\mathcal{X}$ on both sides

$$(\mathcal{X}^n_{\alpha\beta})^* = \Pi^{(0)}(\alpha, \beta^{-1}; \varepsilon^\pi_n) \sum_{\epsilon\theta} \left\langle \alpha\beta^{-1} \right| V_{ph} \left| \epsilon\theta^{-1} \right\rangle (\mathcal{X}^n_{\epsilon\theta})^*. \tag{14.27}$$

The summation over the quantum numbers ϵ and θ is restricted to either ph or hp combinations as can be inferred from the contributions that are obtained by iteration employing $\Pi^{(0)}$. The external quantum numbers α and β similarly can correspond to a ph or a hp combination. In the case that $\alpha > F$ and $F > \beta$ one may write Eq. (14.27) as follows

$$\{\varepsilon^\pi_n - (\varepsilon_\alpha - \varepsilon_\beta)\} (\mathcal{X}^n_{\alpha\beta})^* = \sum_{\epsilon\theta} \left\langle \alpha\beta^{-1} \right| V_{ph} \left| \epsilon\theta^{-1} \right\rangle (\mathcal{X}^n_{\epsilon\theta})^*, \tag{14.28}$$

whereas in the case $F > \alpha$ and $\beta < F$ one has

$$\{\varepsilon^\pi_n + (\varepsilon_\beta - \varepsilon_\alpha)\} (\mathcal{X}^n_{\alpha\beta})^* = -\sum_{\epsilon\theta} \left\langle \alpha\beta^{-1} \right| V_{ph} \left| \epsilon\theta^{-1} \right\rangle (\mathcal{X}^n_{\epsilon\theta})^*. \tag{14.29}$$

Equations (14.28) and (14.29) together form a nonhermitian eigenvalue problem with important consequences since there is no guarantee that all eigenvalues will be real. Before discussing the circumstances of the appearance of complex eigenvalues and their physical relevance, it is useful to introduce the folowing matrix notation for the eigenvalue problem of Eqs. (14.28) and (14.29)

$$\begin{pmatrix} A & B \\ -B' & -A' \end{pmatrix} \begin{pmatrix} (\mathcal{X}_>)^* \\ (\mathcal{X}_<)^* \end{pmatrix} = \varepsilon^\pi \begin{pmatrix} (\mathcal{X}_>)^* \\ (\mathcal{X}_<)^* \end{pmatrix}, \tag{14.30}$$

where the various ingredients are defined as follows. The matrix A has matrix elements

$$A \Rightarrow \delta_{\alpha\epsilon}\delta_{\beta\theta}(\varepsilon_\alpha - \varepsilon_\beta) + \left\langle \alpha\beta^{-1} \right| V_{ph} \left| \epsilon\theta^{-1} \right\rangle, \tag{14.31}$$

where both α and ϵ refer to empty and β and θ to occupied states. The matrix B is given by

$$B \Rightarrow \left\langle \alpha\beta^{-1} \right| V_{ph} \left| \epsilon\theta^{-1} \right\rangle, \tag{14.32}$$

where now α and θ refer to particle and β and ϵ to hole states. Similarly,

$$B' \Rightarrow \left\langle \alpha\beta^{-1} \right| V_{ph} \left| \epsilon\theta^{-1} \right\rangle , \tag{14.33}$$

with α and θ refer to hole and β and ϵ to particle states. Finally,

$$A' \Rightarrow \delta_{\alpha\epsilon}\delta_{\beta\theta}(\varepsilon_\beta - \varepsilon_\alpha) + \left\langle \alpha\beta^{-1} \right| V_{ph} \left| \epsilon\theta^{-1} \right\rangle , \tag{14.34}$$

where both α and ϵ refer to occupied and β and θ to empty states. In many cases it is appropriate to consider a ph space with finite dimension D so that Eq. (14.30) (or the combination of Eqs. (14.28) and (14.29)) has dimension 2D. We note that this eigenvalue problem is nonhermitian which yields interesting consequences discussed below.

To illustrate the properties of this type of eigenvalue problem, it is quite instructive to consider the simplified case where the ph interaction is separable in the following way

$$\left\langle \alpha\beta^{-1} \right| V_{ph} \left| \epsilon\theta^{-1} \right\rangle = \chi Q^*_{\alpha\beta} Q_{\epsilon\theta}, \tag{14.35}$$

where χ is a coupling constant. Substitution of Eq. (14.35) into Eqs. (14.28) and (14.29) then yields

$$\left\{\varepsilon^\pi_n - (\varepsilon_\alpha - \varepsilon_\beta)\right\} (\mathcal{X}^n_{\alpha\beta})^* = \chi Q^*_{\alpha\beta} \sum_{\epsilon\theta} Q_{\epsilon\theta} (\mathcal{X}^n_{\epsilon\theta})^*, , \tag{14.36}$$

for $\alpha > F, F > \beta$ and

$$\left\{\varepsilon^\pi_n + (\varepsilon_\beta - \varepsilon_\alpha)\right\} (\mathcal{X}^n_{\alpha\beta})^* = -\chi Q^*_{\alpha\beta} \sum_{\epsilon\theta} Q_{\epsilon\theta} (\mathcal{X}^n_{\epsilon\theta})^*. \tag{14.37}$$

for the case $F > \alpha$ and $\beta < F$. This implies that

$$(\mathcal{X}^n_{\alpha\beta})^* = \mathcal{N} \frac{Q^*_{\alpha\beta}}{\varepsilon^\pi_n - (\varepsilon_\alpha - \varepsilon_\beta)} \tag{14.38}$$

for $\alpha > F$ and $\beta < F$ but

$$(\mathcal{X}^n_{\alpha\beta})^* = -\mathcal{N} \frac{Q^*_{\alpha\beta}}{\varepsilon^\pi_n - (\varepsilon_\alpha - \varepsilon_\beta)} \tag{14.39}$$

when $F > \alpha$ and $\beta > F$. The constant $\mathcal{N}$ is given by

$$\mathcal{N} = \chi \sum_{\epsilon\theta} Q_{\epsilon\theta} (\mathcal{X}^n_{\epsilon\theta})^*, \tag{14.40}$$

where the sum extends over both ph and hp combinations. One may now insert the solutions for the transition amplitudes given by Eqs. (14.38) and

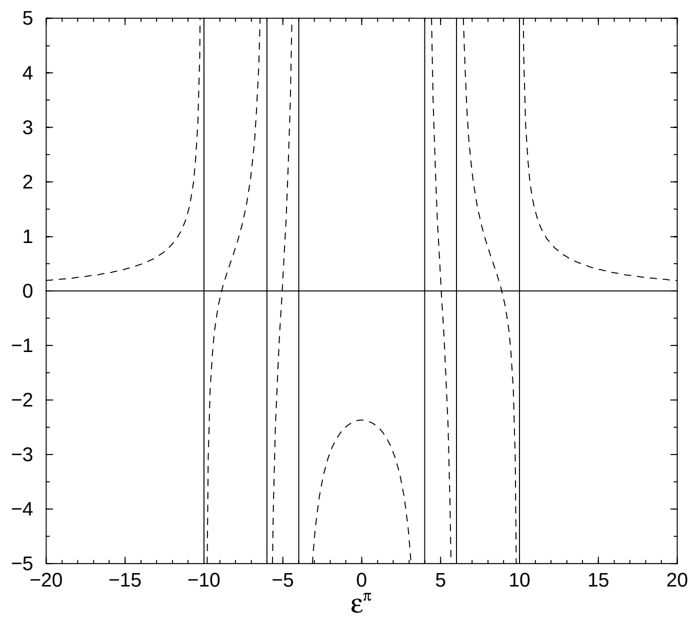

Fig. 14.7 Graphical representation of the right hand side of Eq. (14.41).

(14.39) into Eq. (14.36) to obtain after cancelling the common factors on both sides and dividing by χ

$$\frac{1}{\chi} = \sum_{\epsilon > F, \theta < F} \frac{|Q_{\epsilon\theta}|^2}{\varepsilon_n^\pi - (\varepsilon_\epsilon - \varepsilon_\theta)} - \sum_{\epsilon < F, \theta > F} \frac{|Q_{\epsilon\theta}|^2}{\varepsilon_n^\pi - (\varepsilon_\epsilon - \varepsilon_\theta)}. \tag{14.41}$$

The only unknowns in this equation correspond to the set of eigenvalues ε^π that yield a solution to this equation. One naturally expects the number of these solution to correspond to 2D. The properties of these eigenvalues can be understood by plotting the right hand side of Eq. (14.41) as a function of the energy variable ε^π. Assuming for illustration purposes only 3 ph states a corresponding plot plot is given in Fig. 14.7. The structure of this plot is very illustrative and follows a specific pattern. In Fig. 14.7 the location of the poles in Eq. (14.41) is illustrated by the vertical asymptotes which are located symmetrically about 0 at $\pm$ the ph energies. At negative energies smaller than the location of leftmost pole the second sum in Eq. (14.41) dominates (since its poles are closer) and yields a positive contribution which increases from zero to ∞ when the leftmost pole is reached. Beyond this first pole but before the next one, the function traverses all values starting from $-\infty$ to ∞. This type of behavior would continue for any number of discrete poles until one passes the last pole at negative energies. In this region until the first pole at positive energies the function is negative definite. After the first pole and before the second at positive energy, the function goes from ∞ to $-\infty$ and so on. After the last pole at positive energy the function is again positive definite and approaches zero for large energies. The location of the eigenvalues is very easy to obtain graphically by drawing the straight line corresponding to $1/\chi$ corresponding to the left side of Eq. (14.41). The eigenvalues then simply correspond to the energies at which this straight line intersects with the dashed line in Fig. 14.7. Is is useful to distinguish between a repulsive ($\chi > 0$) and attractive interaction ($\chi < 0$). If the interaction is repulsive the solutions at positive energy will first be found between the unperturbed ph energies. These first D-1 solutions are trapped between the unperturbed ph energies. The last solution is found above the last unperturbed ph energy. In the limit that the interaction becomes weak, $1/\chi$ becomes large and all solutions will tend to the original ph energies. If the interaction is very strong the straight line representing $1/\chi$ will approach zero and the solution above the last unperturbed ph energy may become very large. The latter state will have very collective features to be discussed below in more detail.

For an attractive interaction, one also finds D-1 solutions in between the unperturbed ph energies. For a small value of $|\chi|$ another solution will be found below the lowest unperturbed energy. However, if the strength of $|\chi|$ is increased, this solution will tend to zero excitation energy. Increasing $|\chi|$ further, this solution will disappear when the straight line representing $1/\chi$ no longer crosses the dashed line between zero and this first ph energy. At this point two complex eigenvalues will emerge as will be illustrated below. The appearance of these complex eigenvalues (conjugate pair) signals a characteristic instability that is inherent in the RPA eigenvalue problem. Clearly, it signals the situation when one obtains a negative excitation energy corresponing to an unphysical situation. The corresponding time evolution of these solutions has a component that will exponentially increase and cannot represent a true excited state. Indeed, the instability indicates that the ground state is unstable with respect to this type of collective excitation. This situation can often be repaired by considering the contribution of such collective excitations to the self-energy as discussed in Ch. 16. This instability does not appear if the backward-going part of the unperturbed ph propagator is neglected in the eigenvalue problem. This case simply corresponds to eliminating the summation pover hp states in Eqs. (14.36), (14.37), and (14.41). In that case, the poles at negative energy in Fig. 14.7 disappear and the dashed line approaches zero from below at negative energies. This implies that the lowest solution to this eigenvalue problem in the case of an attractive interaction can be found at a negative excitation energy, a physically unrealistic situation. This approximation to the polarization propagator is known as the Tamm-Dancoff approximation (TDA). This approximation is completely equivalent to a diagonalization of the ph interaction in the chosen basis of ph states as can be inferred from Eq. (14.36) or the more general Eq. (14.28). We note that the contribution of the backward-going terms becomes as important as the forward-going terms when ε^π approaches zero which is reflected in the values of the corresponding $\mathcal{X}$ coefficients.

The character of the eigenvectors associated with the solutions discussed above can be inferred by considering Eqs. (14.38) and (14.39). While these solutions still require normalization, it is clear that for a weak interaction when the eigenvalues remain close to the unperturbed ones, the eigenvector will be dominated by the corresponding unperturbed ph state belonging to that energy. In addition, the admixture of hp amplitudes $(\mathcal{X}_<)^*$ is also small since the corresponding amplitudes (Eq. (14.39) are even further removed in energy. It should also be noted that these amplitudes are strictly zero for the unperturbed case. It is possible to get explicit results for the collective state when one takes the limit in which all unperturbed ph energies are degenerate. Defining

$$\mathcal{C} = \sum_{\epsilon>F,\theta<F} |Q_{\epsilon\theta}|^2 \tag{14.42}$$

and denoting the degenerate ph energy by ε_{ph}, the eigenvalue problem simplifies to

$$\frac{1}{\chi} = \mathcal{C}\left\{\frac{1}{\varepsilon^\pi - \varepsilon_{ph}} - \frac{1}{\varepsilon^\pi + \varepsilon_{ph}}\right\}. \tag{14.43}$$

Again D-1 solutions (at positive energy) will remain trapped at ε_{ph} but one will correspond to the positive solution of Eq. (14.43). This solution then reads

$$\varepsilon^\pi = \left[2\chi\mathcal{C}\varepsilon_{ph} + \varepsilon_{ph}^2\right]^{1/2}. \tag{14.44}$$

This collective state which moves up or down from the unperturbed ph energy ε_{ph} depending on the sign of χ, can have a very different energy from ε_{ph} depending on whether $|\chi|$ is large or not. Only in the case $\chi < 0$ can an imaginary root appear since $\mathcal{C}$ is a positive definite quantity.

The notion of a collective state can be further elaborated by considering the transition probability for the operator (summing over $\overline{\beta}$ is equivalent to summing over β)

$$\hat{Q} = \sum_{\alpha\overline{\beta}} Q_{\alpha\overline{\beta}} a_\alpha^\dagger a_{\overline{\beta}}. \tag{14.45}$$

The corresponding transition probability to the state with energy ε^π in Eq. (14.44) can be shown to become

$$\left| \left\langle \Psi_n^A \right| \hat{Q} \left| \Psi_0^A \right\rangle \right|^2 = \frac{\varepsilon_{ph}}{\varepsilon^\pi} \mathcal{C}. \tag{14.46}$$

To demonstrate this result one must make use of the normalization condition for each solution n

$$\sum_{\alpha>F,\beta<F} |\mathcal{X}_{\alpha\beta}^n|^2 - \sum_{\alpha<F,\beta>F} |\mathcal{X}_{\alpha\beta}^n|^2 = 1 \tag{14.47}$$

which can be obtained in the standard fashion. In this extreme limit all the transition strength combines into this one collective state. In particular in the case of strong attraction when ε^π approaches zero, one may have an extremely large transition probability. Nuclei with even numbers of protons and neutrons in the middle of major shells show enhancements of the quadrupole transition probability that exceed the sp estimate by more than the number of nucleons. Indeed, it is clear from Eq. (14.46) that the size of this constructive interference is not limited in principle.

14.4 Excited states in atoms

14.5 Polarization propagator in infinite systems

The polarization propagator in an infinite system with translational invariance is diagonal in the total momentum of the ph pair. This is similar to the situation for the sp propagator which is also diagonal in momentum space as discussed in Ch. 11. The addition of a ph pair in an infinite system corresponds for example to the addition of a particle with momentum $\boldsymbol{p}_\gamma$ and the addition of a hole with $\boldsymbol{p}_\delta$. In the case this pair is added to the noninteracting ground state, one has

$$\begin{aligned}\left|\gamma,\delta^{-1}\right\rangle &= a^{\dagger}_{\boldsymbol{p}_\gamma,m_\gamma} b^{\dagger}_{\boldsymbol{p}_\delta,m_\delta}\left|\Phi_0^A\right\rangle \\ &= a^{\dagger}_{\boldsymbol{p}_\gamma,m_\gamma}(-1)^{1/2+m_\delta} a_{-\boldsymbol{p}_\delta,-m_\delta}\left|\Phi_0^A\right\rangle . \end{aligned} \tag{14.48}$$

Since removing $-\boldsymbol{p}_\delta$ is equivalent to adding momentum $\boldsymbol{p}_\delta$ and the initial state has no momentum, the new ph state has total momentum

$$\boldsymbol{q}' = \boldsymbol{p}_\gamma + \boldsymbol{p}_\delta . \tag{14.49}$$

Since the Hamiltonian commutes with the total momentum, interactions will not be able to change this momentum $\boldsymbol{q}'$. As a result, the polarization propagator can be labeled with this conserved quantity since after propagation the return to the ground state will have to correspond to the removal of another ph pair carrying the same total momentum. It is therefore convenient to rewrite the polarization propagator given by Eq. (14.7) using the following momentum variables

$$\boldsymbol{q} = \boldsymbol{p}_\alpha + \boldsymbol{p}_\beta \tag{14.50}$$

$$\boldsymbol{p} = \frac{1}{2}\left(\boldsymbol{p}_\alpha - \boldsymbol{p}_\beta\right) \tag{14.51}$$

corresponding to $\alpha\beta^{-1}$ with $\boldsymbol{q}$ being necessarily equal to the total momentum given by Eq. (14.49). Introducing also

$$\boldsymbol{p}' = \frac{1}{2}\left(\boldsymbol{p}_\gamma - \boldsymbol{p}_\delta\right), \tag{14.52}$$

one may consider the momenta $\boldsymbol{p}$ and $\boldsymbol{p}'$ as the relative ph momenta corresponding to $\alpha\beta^{-1}$ and $\gamma\delta^{-1}$, respectively. Using this convention for the noninteracting polarization propagator one may write

$$\begin{aligned}&\Pi^{(0)}(\alpha,\beta^{-1};\gamma,\delta^{-1};E) \Rightarrow \\ &\quad \Pi^{(0)}(\boldsymbol{p}_\alpha m_\alpha,(\boldsymbol{p}_\beta m_\beta)^{-1};\boldsymbol{p}_\gamma m_\gamma,(\boldsymbol{p}_\delta m_\delta)^{-1};E) \\ &\qquad \equiv \delta_{m_\alpha,m_\gamma}\delta_{m_\beta,m_\delta}\delta_{\boldsymbol{q},\boldsymbol{q}'}\delta_{\boldsymbol{p},\boldsymbol{p}'}\Pi^{(0)}(\boldsymbol{p};\boldsymbol{q},E), \end{aligned} \tag{14.53}$$

where

$$\begin{aligned}\Pi^{(0)}(\boldsymbol{p};\boldsymbol{q},E) = &\left\{ \frac{\theta(|\boldsymbol{p}+\boldsymbol{q}/2|-p_F)\theta(p_F-|\boldsymbol{q}/2-\boldsymbol{p}|)}{E-(\varepsilon(\boldsymbol{p}+\boldsymbol{q}/2)-\varepsilon(\boldsymbol{q}/2-\boldsymbol{p}))+i\eta}\right. \\ &\left. - \frac{\theta(p_F-|\boldsymbol{p}+\boldsymbol{q}/2|)\theta(|\boldsymbol{q}/2-\boldsymbol{p}|-p_F)}{E+(\varepsilon(\boldsymbol{q}/2-\boldsymbol{p})-\varepsilon(\boldsymbol{p}+\boldsymbol{q}/2))-i\eta}\right\}, \end{aligned} \tag{14.54}$$

where the remaining sp quantum numbers like spin (and/or isospin) have been kept explicitly and are denoted generically by m_α, m_β, etc. The Kronecker deltas identify all the relevant conserved quantities including the relative momentum. In general, the interaction can change spins (isospins) and the relative momentum. So for the exact polarization propagator one may only make the replacement

$$\Pi(\alpha,\beta^{-1};\gamma,\delta^{-1};E) \Rightarrow \Pi(\boldsymbol{p}_\alpha m_\alpha,(\boldsymbol{p}_\beta m_\beta)^{-1};\boldsymbol{p}_\gamma m_\gamma,(\boldsymbol{p}_\delta m_\delta)^{-1};E) \\ \equiv \delta_{\boldsymbol{q},\boldsymbol{q}'}\Pi(\boldsymbol{p},m_\alpha,m_\beta^{-1};\boldsymbol{p}',m_\gamma,m_\delta^{-1};\boldsymbol{q},E). \quad (14.55)$$

These considerations also apply to the RPA approximation to the polarization propagator so that one may write Eq. (14.20) as

$$\Pi^{RPA}(\boldsymbol{p},m_\alpha,m_\beta^{-1};\boldsymbol{p}',m_\gamma,m_\delta^{-1};\boldsymbol{q},E) = \delta_{m_\alpha,m_\gamma}\delta_{m_\beta,m_\delta}\delta_{\boldsymbol{p},\boldsymbol{p}'} \\ \times \Pi^{(0)}(\boldsymbol{p};\boldsymbol{q},E) + \Pi^{(0)}(\boldsymbol{p};\boldsymbol{q},E)\sum_{\boldsymbol{p}''}\sum_{m_\epsilon m_\theta}\langle \boldsymbol{q},\boldsymbol{p};m_\alpha m_\beta^{-1}|V_{ph}\left|\boldsymbol{q},\boldsymbol{p}'';m_\epsilon m_\theta^{-1}\right\rangle \\ \times \Pi^{RPA}(\boldsymbol{p}'',m_\epsilon,m_\theta^{-1};\boldsymbol{p}',m_\gamma,m_\delta^{-1};\boldsymbol{q},E), \quad (14.56)$$

where momentum conservation has been taken into account.

Uncoupled ph states correspond to the result of Eq. (14.48) and can be written in terms of the momentum variables $\boldsymbol{q},\boldsymbol{p}$ as

$$|\boldsymbol{q},\boldsymbol{p};m_\alpha,m_\beta^{-1}\rangle = a^\dagger_{\boldsymbol{p}+\boldsymbol{q}/2,m_\alpha} b^\dagger_{\boldsymbol{q}/2-\boldsymbol{p},m_\beta}\left|\Phi_0^A\right\rangle. \quad (14.57)$$

In principle one can consider the quantum numbers m_α and m_β to include isospin. Specializing for now to the case of spin only, the coupled states are obtained by employing the usual Clebsch-Gordan coefficients

$$|\boldsymbol{q},\boldsymbol{p};S,M_S\rangle = \sum_{m_\alpha,m_\beta}\left(\tfrac{1}{2}\ m_\alpha\ \tfrac{1}{2}\ m_\beta \mid S\ M_S\right)\ |\boldsymbol{q},\boldsymbol{p};m_\alpha,m_\beta^{-1}\rangle. \quad (14.58)$$

With these preliminaries it is clear the polarization propagator with good total spin requires the usage of the corresponding hole operators combined with the appropriate Clebsch-Gordan summations. The corresponding coupled propagator can then be written as

$$\Pi(\boldsymbol{p},S,M_S;\boldsymbol{p}',S',M_S';\boldsymbol{q},E) = \sum_{m_\alpha,m_\beta,m_\gamma,m_\delta}\left(\tfrac{1}{2}\ m_\alpha\ \tfrac{1}{2}\ m_\beta \mid S\ M_S\right) \\ \times\ \left(\tfrac{1}{2}\ m_\gamma\ \tfrac{1}{2}\ m_\delta \mid S'\ M_S'\right)\ \Pi(\boldsymbol{p},m_\alpha,m_\beta^{-1};\boldsymbol{p}',m_\gamma,m_\delta^{-1};\boldsymbol{q},E). \quad (14.59)$$

The possibility of changing the total spin has been kept open in Eq. (14.59). This issue depends on the character of the ph interaction. Before considering the RPA equation in more detail, it is therefore useful to construct the relevant ph matrix elements of the interaction in a coupled spin (isospin) basis. The matrix elements can be coupled to total ph spin in the following way

$$\begin{aligned}
&\langle \boldsymbol{q}, \boldsymbol{p}; S, M_S |\, V_{ph}\, | \boldsymbol{q}, \boldsymbol{p}'; S', M_S' \rangle = \\
&\sum_{m_\alpha, m_\beta, m_\gamma, m_\delta} \left(\tfrac{1}{2}\ m_\alpha\ \tfrac{1}{2}\ m_\beta \mid S\ M_S \right) \left(\tfrac{1}{2}\ m_\gamma\ \tfrac{1}{2}\ m_\delta \mid S'\ M_S' \right) \\
&\qquad \times \langle \boldsymbol{q}, \boldsymbol{p}; m_\alpha, m_\beta^{-1} | V_{ph} \left| \boldsymbol{q}, \boldsymbol{p}'; m_\gamma, m_\delta^{-1} \right\rangle
\end{aligned} \tag{14.60}$$

The evaluation of this matrix element depends on the operator character of the two-body interaction V. It is instructive to evaluate Eq. (14.60) using Eq. (14.17) and express the latter matrix elements also with good total spin. We will proceed by assuming that V corresponds to a local, central interaction without spin dependence but this restriction is by no means necessary as shown in Sec. 14.7. Interactions like the Coulomb interaction given by Eq. (11.90) or interactions of Yukawa-type as in Eqs. (4.20) and (4.33) correspond to this choice and exhibit a simple dependence on the momentum transfer when considered in momentum space. For the contribution of the direct term in Eq. (14.60) this momentum transfer is equal to $\boldsymbol{q}$ the conserved total ph momentum. This direct matrix element therefore does not generate any dependence on the momentum variables $\boldsymbol{p}$ and $\boldsymbol{p}'$. The corresponding contribution to Eq. (14.60) can then be written as

$$\begin{aligned}
&\langle \boldsymbol{q}, \boldsymbol{p}; S, M_S |\, V_{ph}\, | \boldsymbol{q}, \boldsymbol{p}'; S', M_S' \rangle_D = \\
&\sum_{m_\alpha, m_\beta, m_\gamma, m_\delta} \sum_{S_p, M_p} \left(\tfrac{1}{2}\ m_\alpha\ \tfrac{1}{2}\ m_\beta \mid S\ M_S \right) \left(\tfrac{1}{2}\ m_\gamma\ \tfrac{1}{2}\ m_\delta \mid S'\ M_S' \right) \\
&\qquad \times \left(\tfrac{1}{2}\ m_\alpha\ \tfrac{1}{2}\ -m_\delta \mid S_p\ M_p \right) \left(\tfrac{1}{2}\ -m_\beta\ \tfrac{1}{2}\ m_\gamma \mid S_p\ M_p \right) \\
&\qquad \times (-1)^{1/2+m_\beta} (-1)^{1/2+m_\delta}\ V(\boldsymbol{q}),
\end{aligned} \tag{14.61}$$

using the fact that this coupled direct matrix element is diagonal in the total spin and its projection and does not depend on the value of the total spin either. It is conventional to label the latter coupling scheme by particle-particle to contract it with the ph coupling involved in Eq. (14.60). Hence the subscript p is used in Eq. (14.61). The summation over the spin projections in Eq. (14.61) yields a so-called $6j$-symbol (see Appendix C [Messiah (1999)]) while forcing $S = S'$ and $M_S = M_S'$. These $6j$-symbols also occur in the recoupling of three angular momenta and some are tabulated in [Lindgren and Morrison (1982)]. The resulting direct ph matrix element is given by

$$\langle \boldsymbol{q},\boldsymbol{p};S,M_S|\,V_{ph}\,|\boldsymbol{q},\boldsymbol{p}';S',M_S'\rangle_D = \delta_{S,S'}\delta_{M_S,M_S'}\sum_{S_p}(-1)^{S_p+1}(2S_p+1)\begin{Bmatrix}\frac{1}{2} & \frac{1}{2} & S\\ \frac{1}{2} & \frac{1}{2} & S_p\end{Bmatrix}\;V(\boldsymbol{q}), \tag{14.62}$$

where the summation over M_p yields the factor $2S_p+1$. The relevant $6j$-symbols for the S, S_p combinations involve the pairs (0,0), (1,0), (0,1), and (1,1). These $6j$-symbols are given by, $-\frac{1}{2}, \frac{1}{2}, \frac{1}{2}$, and $\frac{1}{6}$, respectively. Inserting these results and performing the sum over S_p one finally obtains the simple result

$$\langle \boldsymbol{q},\boldsymbol{p};S,M_S|\,V_{ph}\,|\boldsymbol{q},\boldsymbol{p}';S',M_S'\rangle_D = \delta_{S,S'}\delta_{M_S,M_S'}\;\delta_{S,0}\;2\;V(\boldsymbol{q}) \tag{14.63}$$

showing that the direct contribution of this type of interaction only contributes when the ph spin $S=0$. From the diagrammatic content of this contribution this makes sense since the total spin of the initial ph state must carried over to the final ph state by the interaction which does not contain spin operators and therefore only selects the $S=0$ channel. The result for a spin-spin interaction considered in Ch. 5 correspondingly only yields a contribution for this direct ph matrix element for total $S=1$. For the exchange term one can proceed in similar fashion but this term yields a contribution to both total $S=0$ and 1. Combining these results and noting that only ph matrix elements survive which are diagonal in the total spin and its projection, one obtains for the final result (with adapted notation)

$$\langle \boldsymbol{q},\boldsymbol{p}|\,V_{ph}^{SM_S}\,|\boldsymbol{q},\boldsymbol{p}'\rangle = \delta_{S,0}\;2\;V(\boldsymbol{q}) - V(\boldsymbol{p}-\boldsymbol{p}'). \tag{14.64}$$

The exchange term of the Coulomb interaction will therefore yield the only contribution when the ph spin is 1 and this contribution is attractive. For other types of interactions including spin (isospin) dependence one can obtain corresponding results by following similar steps. In general, the total ph spin is conserved although in the case of a tensor interaction one must choose the quantization axis judiciously to ensure that the different components do not mix. This will be further discussed in Sec. 14.6.

It is now possible to present the RPA equation in the coupled spin format. By performing the relevant coupling of the ph spins one obtains

$$\Pi^{RPA}(\boldsymbol{p},\boldsymbol{p}';S,M_S,\boldsymbol{q},E) = \delta_{\boldsymbol{p},\boldsymbol{p}'}\Pi^{(0)}(\boldsymbol{p};\boldsymbol{q},E) + \Pi^{(0)}(\boldsymbol{p};\boldsymbol{q},E)\sum_{\boldsymbol{p}''}\langle \boldsymbol{q},\boldsymbol{p}|\,V_{ph}^{SM_S}\,|\boldsymbol{q},\boldsymbol{p}''\rangle\;\Pi^{RPA}(\boldsymbol{p}'',\boldsymbol{p}';S,M_S,\boldsymbol{q},E), \tag{14.65}$$

where the conservation of the total spin and its projection has been incorporated (also in the notation). This integral equation can be simplified considerably in the case that the direct ph matrix element is much more important than the exchange term. This is the case for the Coulomb interaction where the direct term involves the q^{-2} divergence whereas in the exhange term this divergence is essentially integrated away by the implied $\boldsymbol{p}''$ integral in Eq. (14.65). Most applications of this integral equation therefore involve simplifications which make the ph interaction effectively only dependent on $\boldsymbol{q}$. In that case Eq. (14.65) is no longer an integral equation. The corresponding simplification is obtained by considering

$$\Pi^{RPA}_{SM_S}(\boldsymbol{q},E) \equiv \sum_{\boldsymbol{p}} \sum_{\boldsymbol{p}'} \Pi^{RPA}(\boldsymbol{p},\boldsymbol{p}';S,M_S,\boldsymbol{q},E) \tag{14.66}$$

and

$$\Pi^{(0)}(\boldsymbol{q},E) \equiv \sum_{\boldsymbol{p}} \Pi^{(0)}(\boldsymbol{p};\boldsymbol{q},E). \tag{14.67}$$

Using these definitions one can transform Eq. (14.65) into

$$\Pi^{RPA}_{SM_S}(\boldsymbol{q},E) = \Pi^{(0)}(\boldsymbol{q},E) + \Pi^{(0)}(\boldsymbol{q},E)\; V^{SM_S}_{ph}(\boldsymbol{q})\; \Pi^{RPA}_{SM_S}(\boldsymbol{q},E). \tag{14.68}$$

Applications of this equation will be discussed below. Clearly, the first task in order to study Eq. (14.68) is to evaluate the quantity (sometimes called the Lindhard function) $\Pi^{(0)}(\boldsymbol{q},E)$. Replacing the sum over $\boldsymbol{p}$ by an integration according to Eq. (5.10), one obtains

$$\begin{aligned}\Pi^{(0)}(\boldsymbol{q},E) = V \int \frac{d\boldsymbol{p}}{(2\pi\hbar)^3} \Bigg\{ &\frac{\theta(|\boldsymbol{p}+\boldsymbol{q}/2| - p_F)\theta(p_F - |\boldsymbol{p}-\boldsymbol{q}/2|)}{E - (\varepsilon(\boldsymbol{p}+\boldsymbol{q}/2) - \varepsilon(\boldsymbol{q}/2-\boldsymbol{p})) + i\eta} \\ &- \frac{\theta(p_F - |\boldsymbol{p}+\boldsymbol{q}/2|)\theta(|\boldsymbol{p}-\boldsymbol{q}/2| - p_F)}{E + (\varepsilon(\boldsymbol{q}/2-\boldsymbol{p}) - \varepsilon(\boldsymbol{p}+\boldsymbol{q}/2)) - i\eta} \Bigg\}. \end{aligned} \tag{14.69}$$

Equation (14.69) can be evaluated analytically as will be illustrated here for the imaginary part explicitly. For the description of excited states only the case $E > 0$ need be considered. Using the identity of Eq. (8.16) one must consider only the contribution of the first term in Eq. (14.69) for the imaginary part

$$\begin{aligned}\mathrm{Im}\ \Pi^{(0)}(\boldsymbol{q},E) = -\pi V \int \frac{d\boldsymbol{p}}{(2\pi\hbar)^3} \qquad\qquad (14.70)\\ \times\ \theta(|\boldsymbol{p}+\boldsymbol{q}/2| - p_F)\theta(p_F - |\boldsymbol{p}-\boldsymbol{q}/2|)\delta(E - (\varepsilon(\boldsymbol{p}+\boldsymbol{q}/2) - \varepsilon(\boldsymbol{p}-\boldsymbol{q}/2)).\end{aligned}$$

In order to evaluate this expression one first considers the momentum dependence of the ph energy difference in the argument of the δ function

$$\varepsilon(\boldsymbol{p}+\boldsymbol{q}/2)-\varepsilon(\boldsymbol{p}-\boldsymbol{q}/2)=\frac{\boldsymbol{p}\cdot\boldsymbol{q}}{m}=\frac{p\ q\ \cos\theta}{m}. \qquad (14.71)$$

If $\boldsymbol{q}$ is chosen along the z-axis, $p\cos\theta = p_z$ and energy conservation corresponds to

$$E=\frac{p_z q}{m}, \qquad (14.72)$$

showing that energy conservation (and the accompanying imaginary part of $\Pi^{(0)}$) corresponds to fixed values of p_z. It is now useful to distinguish two cases for the total ph momentum. This distinction arises from the consideration of the two step functions in Eq. (14.70). In the space corresponding to the integration variable $\boldsymbol{p}$ these conditions are respresented by two spheres with radius p_F, one displaced from the origin by $\boldsymbol{q}/2$, the other by $-\boldsymbol{q}/2$. The step function pertaining to the hole then requires only consideration of values of $\boldsymbol{p}$ inside the first sphere while the other step function only allows values outside the second sphere as indicated in Fig. 14.8. Since these two spheres are displaced from each other by q, they no longer overlap for $q > 2p_F$ so it is useful to distinguish between the corresponding two cases. Consider first the case $q > 2p_F$ when the spheres don't overlap and the step functions allow all values of $\boldsymbol{p}$ inside the top sphere in Fig 14.8. Energy conservation in the form of Eq. (14.72) shows that a minimum and maximum energy exist corresponding to p_z touching the bottom corresponding to $p_z = q/2 - p_F$ and the top of the allowed sphere where $p_z = q/2 + p_F$, respectively. These conditions translate to a nonvanishing of the imaginary part of $\Pi^{(0)}$ when

$$\frac{q^2}{2m}-\frac{qp_F}{m}<E<\frac{q^2}{2m}+\frac{qp_F}{m}. \qquad (14.73)$$

It is now straightforward to perform the integrations in Eq. (14.70). The integration over the azimuth angle give a factor of 2π, while the $\cos\theta$ intergration is taken care of by the δ function employing the following property

$$\delta\left(E-\frac{p\ q}{m}\cos\theta\right)=\frac{m}{pq}\ \delta\left(\frac{mE}{p\ q}-\cos\theta\right). \qquad (14.74)$$

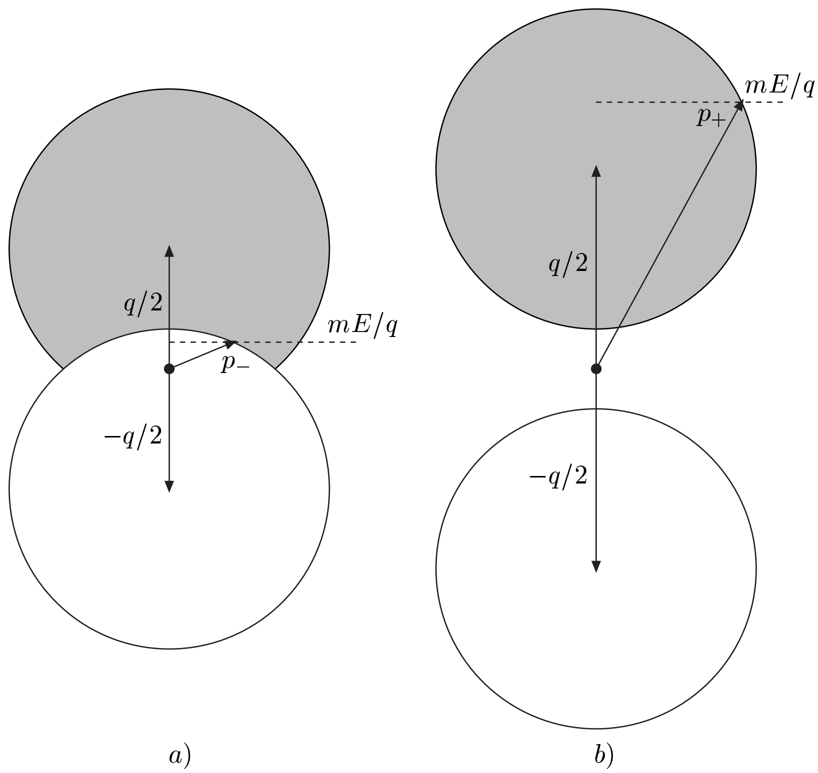

Fig. 14.8 Illustration of the contraints imposed by the step functions in Eq. (14.70). The condition $|\boldsymbol{p}+\boldsymbol{q}/2| > p_F$ corresponds to the area outside the lower sphere in both figures while the condition $|\boldsymbol{p}-\boldsymbol{q}/2| < p_F$ only allows contributions from inside the top sphere. Part a) illiustrates the case when $q < 2p_F$ when these spheres overlap while b) is appropriate for $q > 2p_F$ when there is no overlap. The gray area indicates the allowed region for the integration over $\boldsymbol{p}$. The dashed lines in part a) and b) correspond to possible energy values for which a nonzero imaginary part is obtained. The corresponding condition is expressed by Eq. (14.72) which shows that the only contributions to Eq. (14.70) correspond to the part of the dashed line inside the gray area of the top sphere. Some limiting values of the integration variable p in Eq. (14.75) are indicated by the arrows with the corresponding labels.

The final integration over the magnitude of $\boldsymbol{p}$ is then given by

$$\text{Im}\ \Pi^{(0)}(\boldsymbol{q},E) = -\frac{\pi V}{\hbar^3}\frac{2\pi m}{(2\pi)^3 q}\int_{p_-}^{p_+} dp\ p = -\frac{V}{\hbar^3}\frac{m}{8\pi q}\left[p_F^2 - \left(\frac{mE}{q}-\frac{q}{2}\right)^2\right], \tag{14.75}$$

where the lower limit is given by

$$p_- = \frac{mE}{q} \tag{14.76}$$

and the upper limit by

$$p_+ = \left[p_F^2 - q^2/4 + mE\right]^{1/2} \tag{14.77}$$

from the condition which ensures that $|\boldsymbol{p} - \boldsymbol{q}/2| < p_F$.

The case $q < 2p_F$ involves two overlapping spheres illustrated in Fig. 14.8a). For energies E such that $\theta = 0$ is allowed (when the dashed line is above the lower sphere) the same result as in Eq. (14.75) is obtained since one retraces identical steps. This energy domain also corresponds to the upperlimit given in Eq. (14.73). Since the excitation spectrum corresponding to Eq (14.71) starts at zero energy (for $q < 2p_F$) the remaining energy domain corresponds to

$$0 < E < \frac{qp_F}{m} - \frac{q^2}{2m}, \tag{14.78}$$

where the upperlimit corresponds to the energy for which the dashed in Fig. 14.8a) is no longer contrained by the lower sphere. The integrations proceed as before except that the lower limit in Eq. (14.75) is now replaced by

$$p_- = \left[p_F^2 - q^2/4 - mE\right]^{1/2}, \tag{14.79}$$

corresponding to the restriction $|\boldsymbol{p} + \boldsymbol{q}/2| > p_F$. The final result for the imaginary part of the noninteracting polarization propagator then becomes

$$\text{Im}\ \Pi^{(0)}(\boldsymbol{q}, E) = -\frac{V}{\hbar^3}\frac{m}{4\pi q}mE. \tag{14.80}$$

To obtain the real part of $\Pi^{(0)}$ one can proceed by straightforward integration of Eq. (14.69) as in [Fetter and Walecka (1971)]. An alternative procedure may be followed by using Eq. (14.70) and the corresponding result for the imaginary part for $E < 0$ to rewrite Eq. (14.69) in the form of a dispersion integral (see Ch. 13)

$$\begin{aligned}\Pi^{(0)}(\boldsymbol{q}, E) = &-\frac{1}{\pi}\int_{E_-}^{E_+} dE' \frac{\text{Im}\ \Pi^{(0)}(\boldsymbol{q}, E')}{E - E' + i\eta} \\ &+ \frac{1}{\pi}\int_{-E_+}^{-E_-} dE' \frac{\text{Im}\ \Pi^{(0)}(\boldsymbol{q}, E')}{E - E' - i\eta},\end{aligned} \tag{14.81}$$

Fig. 14.9 Illustration of the different shapes associated with the imaginary part of $\Pi^{(0)}$ depending on the magnitude of q. In part a) the case $q < 2p_F$ is considered. Equations (14.78) and (14.80) are multiplied by appropriate factors.

where the energy limits are given by

$$E_- = \begin{cases} 0 & q < 2p_F \\ \dfrac{q^2}{2m} - \dfrac{qp_F}{m} & q > 2p_F \end{cases} \tag{14.82}$$

and

$$E_+ = \frac{q^2}{2m} + \frac{qp_F}{m} \tag{14.83}$$

for any value of q. By simply inserting the values obtained for the imaginary parts of $\Pi^{(0)}$ for $E > 0$ and $E < 0$ from Eq. (14.69) into Eq. (14.81) one recovers the original equation (14.69) confirming the validity of Eq. (14.81). Using the expressions for the imaginary part obtained in Eqs. (14.75) and (14.80) one can evaluate the real part of $\Pi^{(0)}$ also by employing Eq. (14.81). The resulting expression for the real part is given by

$$\begin{aligned} \mathrm{Re}\ \Pi^{(0)}(\boldsymbol{q}, E) = &\frac{V}{\hbar^3}\frac{mp_F}{4\pi^2} \\ \times &\left\{-1 + \frac{p_F}{2q}\left[1 - \left(\frac{mE}{qp_F} - \frac{q}{2p_F}\right)^2\right] \ln\left|\frac{2qp_F + 2mE - q^2}{2qp_F - 2mE - q^2}\right| \right. \\ &\left. -\frac{p_F}{2q}\left[1 - \left(\frac{mE}{qp_F} + \frac{q}{2p_F}\right)^2\right] \ln\left|\frac{2qp_F + 2mE + q^2}{2qp_F - 2mE - q^2}\right| \right\}. \end{aligned} \tag{14.84}$$

A plot for the real and imaginary part of $\Pi^{(0)}$ is shown in Fig. A comparison of the imaginary parts for q below and above $2p_F$ is shown in Fig. 14.9.

The imaginary part of $\Pi^{(0)}$ can be interpreted as the probability to absorb momentum q and energy E by the noninteracting Fermi sea. The shape of this probability as a function of energy for $q > 2p_F$ has the shape of an inverted parabola, the width being proportional to the Fermi momentum. Data for inelastic election scattering from nuclei in this high-momentum domain can be interpreted in this way. Indeed one obtains very reasonable values for the Fermi momentum from such an analysis.

14.6 Plasmons in the electron gas

Ths solution of the RPA equation in an infinite systems in the case of the electron gas has substantial relevance for the global properties of this system. The Coulomb interaction must be used in Eq. (14.64) which therefore reads

$$\langle \boldsymbol{q}, \boldsymbol{p}; S, M_S | V_C | \boldsymbol{q}, \boldsymbol{p}'; S', M_S' \rangle = \delta_{S,S'} \delta_{M_S,M_S'} \frac{4\pi e^2}{V} \left\{ \delta_{S,0} \ \frac{2}{\boldsymbol{q}^2} \ - \frac{1}{|\boldsymbol{p} - \boldsymbol{p}'|^2} \right\}. \quad (14.85)$$

Since the momentum $\boldsymbol{q}$ is conserved, it is clear that the direct term in Eq. (14.85) completely dominates the ph interaction at small values of q. One may therefore expect that the corresponding implementation of the RPA equation which neglects the exchange contribution represents the dominant physics in that limit. As a result, it is permissible to use Eq. (14.68) to solve for the polarization propagator. Denoting the matrix element of V in Eq. (14.85) by $V(q)$ while neglecting the exchange term, the solution to Eq. (14.68) is given by

$$\Pi_{S=0}^{RPA}(q, E) = \frac{\Pi^{(0)}(q, E)}{1 - V(q)\Pi^{(0)}(q, E)}, \quad (14.86)$$

where only the magnitude of $\boldsymbol{q}$ is kept in the notation. The probability for the absorption of momentum q and energy E is again given by the imaginary part of Π^{RPA} and therefore a contribution will be found in the energy domain where the numerator has an imaginary part. This domain is given by Eqs. (14.82) and (14.83). These boundaries are plotted in Fig. 14.10 as a function of q. The special character of the Coulomb interaction, its divergence for $q \to 0$, requires further scrutiny. To appreciate what is happening it is useful to remember the schematic model with attractive and repulsive ph interactions discussed in Sec. 14.3. This discussion for the repulsive case obviously applies here and one may conjecture that a collective state may appear above the region of "trapped" ph energies given by the boundaries

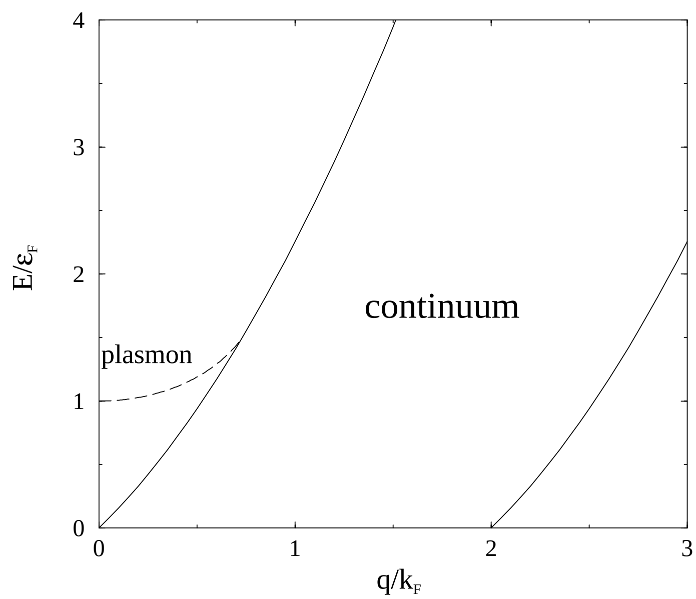

Fig. 14.10 Boundaries of the ph continuum are indicated by the full lines. Plasmon energy as a function of q is shown by the dashed line.

of the imaginary part of $\Pi^{(0)}$. Such a collective state, ususally referred to as a plasmon, will turn up in the Lehmann representation of the polarization propagator as a pole. The condition for the appearance of a pole for a fixed value of q then requires for $E > q^2/2m + qp_F/m$ that the denominator of Eq. (14.86) vanishes for a certain E_p

$$1 - V(q) \text{ Re } \Pi^{(0)}(q, E_p) = 0, \tag{14.87}$$

where the use of the real part emphasizes that in this energy domain the imaginary part of $\Pi^{(0)}$ vanishes. In the language of the solution method previously discussed for propagator equations this result is obtained by assuming a pole in the Lehmann representation for $\Pi^{RPA}_{S=0}$

$$\Pi^{RPA}_{S=0}(q, E) = \frac{\mathcal{C}_p}{E - E_p} + ... \tag{14.88}$$

Inserting this result in Eq. (14.68) and considering energies near the pole E_p leads to the eigenvalue equation for E_p which can be written as Eq. (14.87). Using the small q limit the real part of the noninteracting polarization propagator for a fixed energy E_p, yields the following result for the plasmon energy when this result is inserted in Eq. (14.87)... The result for other values of q is plotted in Fig. 14.10.

14.7 Response of nuclear matter with π and ρ meson quantum numbers

14.8 Excitations of a normal Fermi liquid

14.9 Exercises